ORIGINAL ARTICLE
DOI: 10.4274/tjps.galenos.2020.47897

Development of PLA and BSA layered coated chitosan microneedles using novel bees wax mould

Ravindra V Badhe, Deepak Adkine, Anagha Godse
Dr. D. Y. Patil Institute of Pharmaceutical Sciences and Research, Pimpri, Pune, MS, India
Corresponding Author Information
Ravindra V Badhe
ravindra.badhe@dypvp.edu.in
9422432038
0000-0002-9919-8154
31.03.2020
01.09.2020

Abstract
Objectives: This work illustrates novel method of fabrication of polymeric microneedle (MN) construct using bees wax as mould and development of coated polymeric microneedles for drug delivery.
Materials and Methods: A novel method of microneedle fabrication using bees wax as mould was established. The porous chitosan microneedle arrays were fabricated and coated with polylactic acid (PLA). The optimized MN arrays were then coated with bovine serum albumin (BSA). The MN were then subjected to physiochemical and tensile strength characterization followed by drug release study. The skin penetration and irritation study were performed *in-vivo* in Wister Albino Rats.
Results: The constructed microneedle arrays contain microneedles with 0.9mm length, 600 µm width at the base, 30-60 µm diameter at the tip, and the distance between two needles was 1.5 mm. These microneedles patch was having good mechanical strength (0.72 N/Needle) and tensile strength 15.23 Mpa. The microneedle array patch has 6.26 % swelling index and 98.5% drug release was observed on 50th hr. good penetration and no skin irritation was observed for optimized MN batch.
Conclusion:
Polymeric MN arrays were successfully developed using bees wax mould and were successfully coated with PLA to deliver the protein (BSA) through skin epidermis layer.
Keywords: Microneedles, transdermal drug delivery, coated microneedles, microneedle mould, bees wax, polylactic acid.

1. Introduction

Microneedles (MN) are structures which are of length up to 2 mm with thickness in few microns. Microneedles pierce the skin without pain and deliver drugs on the epidermis. MNs allow delivery of hydrophilic and lipophilic drugs and macro molecular therapeutics through the micro channels that are physically formed by the MN while disrupting the stratum corneum (SC). MNs do not produce pain because they enter up to the dermis layer without stimulating the sensory nerves.[1] The first generations of Microneedles were prepared from metals, organic polymers, glass, silicones as they were aimed to create the micropores into

the skin to facilitate drug, vaccine or protein diffusion in skin.[2] The first patent on MNs based drug delivery has been filed in US in year 1971. At that time MNs were called as 'puncturing projections'. However, the first successful attempt of MNs development was made in 1990s as silicon MNs successfully facilitated the delivery of calcein, through human skin. MNs have shown effectiveness in delivering many therapeutic molecules through biological membranes including sclera, skin and mucosal tissue.[3,4] Microneedles arrays are based on combining advantages of the non-invasive and invasive systems and eliminating their drawbacks.[5] Solid microneedles show the increase in skin permeability for the compounds of size ranging from small molecules to larger molecules as like proteins to nanoparticles.[6-9] The successful delivery of insulin[13] oligonucleotides, desmopressin, human growth hormone.[10-12] and the immune response from transportation of DNA and protein antigens.[14,15] Most microneedles reported were prepared from silicon[16,17] or metal.[18,19] Silicon is mostly used as a common microelectronics industry substrate but; it is costly, fragile, and untested biocompatible material. There are many metals which are cost effective, have good strength and are known to be biocompatible,[20] which are preferred choice for hollow microneedles as it needs good mechanical strength. Research area of polymer microneedles is recently being explored extensively as they provide inexpensive, biocompatible materials that offer good strength because of polymer viscoelasticity.[21-23] In addition, earlier microneedle fabrication methods were expensive and time consuming due to clean room-intensive process.[24]

As an innovative approach of microneedle fabrication, this study was motivated with the aim to formulate microneedles patch using biodegradable polymers and recyclable mould-based fabrication methods. The polymeric microneedles are cost effective, biologically safe, having novel features (such as biocompatibility, dissolvable, swellable, and biodegradable), no cross contamination and precise in large scale production and thus gained importance now a days. Dissolvable Microneedles were also reported, and they were well-known to be prepared from many of biocompatible materials such as bio polymers like hyaluronic acid. Mostly the popular polymers that are used in the fabrication of microneedles are carboxymethyl cellulose (CMC), hydroxy propyl cellulose (HPC), poly lactic acid (PLA), polyglycolic acid, poly lactic-co-glycolic acid (PLGA), poly (vinyl) alcohol, poly- vinylpyrrolidone (PVP).[25-29] In this study, PLA coated chitosan MN array patches were prepared using novel wax-based mould fabrication. The MNs were tested for their mechanical, physicochemical, release of medicament and swelling properties. The wax base mould provides unique advantage of melting and refabricating a mould multiple times precisely to develop reproducible MN.[30,31]

2. Material and method

2.1 Materials

Chitosan (MW 190–310 kDa and degree of deacetylation 85 %), BSA (bovine serum albumin), dichloromethane, acetic acid and bees wax (MP 63 ^{0}C) purchased from High Media, Dorset, UK. Phosphate buffer saline (PBS) solution was obtained from Fischer scientific. Polylactic acid (PLA MW 60,000) was procured from Sigma-Aldrich, Darmstadt, Germany. All the chemicals used were of analytical grade reagent. Microneedle roller purchased from ZGTS Derma Roller® (1 mm), Medsorimpex, sewak park, New Delhi.

2.2 Preparation of mould

Wax based mould is a simple, economic, less time consuming and innovative technique to prepare microneedle. In this technique the microneedle moulds were developed by using a bee's wax. The bees wax (M.P. 63 ^{0}C) was melted and mixed. The liquid wax preparation was poured into a Petri plate and allowed it to cool and solidify at room temperature.[32] The array is prepared by impressing the Derma Roller® (1 mm needle length) on the surface of the solidified wax. The prepared wax mould is placed in a vacuum oven at (-500 mmHg) for 20 min at (37 ^{0}C) for removal of any dust particles and wax debris.

2.3 Fabrication of microneedle patch

The 0.5-3 %w/v chitosan dissolved in 1 %v/v acetic acid solution was used for fabrication of microneedles. The prepared gel was rested overnight and spread over the prepared microneedle wax mould uniformly. Before spreading the care was taken to avoid formation of any air bubbles. After few minutes the microneedle array was placed in a vacuum oven at 37 ^{0}C for 1 day at -550 mmHg pressure. After completion of 1-day period MN array mould is removed from the oven and generated air bubbles were scrapped by using the glass rod and dried for another 1 day at room temperature. After drying, the microneedle patches were pulled out of wax mould and dried in a hot air oven at 70 ^{0}C for 5 hrs. After complete drying of microneedles, the coating is done by polylactic acid solution prepared by dissolving 500 mg of PLA in 5 mL of dichloromethane. The microneedle patch was dipped 20 times in polylactic acid solution until complete coating.[33] After PLA coating, whole MN patch was dried at 60 ^{0}C to completely remove the traces of dichloromethane. This PLA coated chitosan microneedle patch was again coated with BSA by dipping 20 times in the 10 mg/mL BSA solution (BSA was used as representative protein for macromolecules). The microneedle patches were prepared in several batches (A to G batches) as shown in (Table 1).

2.4 Characterization of optimized microneedle array patch

2.4.1 Physical examination of microneedle array by Microscope and Scanning Electron Microscopy (SEM)

MN arrays were observed under compound microscope for preliminary morphological examination. MN arrays were initially mounted on circular disc and morphologically characterized with scanning electron microscope (Hitachi S-2460N, Germany) in high vacuum using ETD detector at 10^{-5} Torr and 15 kV. Each sample was coated with gold using K550 Emitech Sputter coater (Gatan Inc., Pleasanton, CA). Computer software (XT Microscope control, Quanta Oregon, USA) was used to analyse SEM images.[34]

2.4.2 Mechanical testing of MNs arrays

2.4.2.1 Mechanical strength of microneedles

Mechanical strength of MN was studied with a displacement-force test station (Model 921A, Tricor Systems Inc., Elgin, IL, USA). Microneedle array (1×3 cm with 108 MN) was attached to the mount and an axial force was applied at a rate of 1 mm/s. The microneedle array was mounted against a flat, rigid surface perpendicular to the axis of mount movement. The test station measured the compression force needed to move that mount as a function of distance. The study was done in triplicate (n=3).

2.4.2.2 Tensile strength of microneedle arrays

Tensile strength of MN arrays was determined by using texture analyser (TA.XT *plus*, Stable Micro System, United Kingdom). The tensile strength is determined based on maximum load at the time of film rupture. Three strips of MN array were cut 1×5 cm and used for this test. The thickness and breadth of strips were checked and noted at three different sites and average value was taken for calculation. The study was done in triplicate (n=3).
The tensile strength was calculated using formula 1

$$\text{Tensile strength (MPa)} = \frac{\text{(Load at break in gm)}}{\text{(Original width in mm) (Original thickness in mm)}} \times 100 \quad \text{----(1)}$$

2.4.3 Physicochemical characterisation of MNs array

2.4.3.1 Determination of standard and released BSA (from MN array) by SDS-PAGE

The SDS-PAGE was used for determination of standard BSA (66 kD) and released BSA from microneedle array from Franz diffusion cell and was done as per Badhe et.al.[35] The resolving gel used was 9 % and staining was done with Coomassie brilliant blue stain.

2.4.3.2 Determination of chemical integrity of MNs

FTIR absorption spectrum of chitosan, PLA, BSA and BSA coated on PLA coated chitosan MN was analyzed by using a FTIR spectrophotometer (8400S Shimadzu, Japan) over the range 4000-600 cm^{-1}. The baseline correction was carried out using dried potassium bromide. Subsequently, the spectrum of mixture of analyte and potassium bromide was recorded and the peaks belonging to major functional groups were recorded.

2.4.3.3 Thermodynamic evaluation of MNs arrays

DSC analysis was carried out for chitosan, PLA, PLA coated chitosan microneedle and BSA coated on PLA coated chitosan MN array by using DSC7, PerkinElmer, Germany. Sample weights were taken in the range from 5 mg-10 mg. All samples were analysed in scanning mode from 25 ^{0}C to 350 ^{0}C at heating rate of 10 ^{0}C/min. Dry nitrogen gas was purged in during DSC analysis.

2.4.3.4 Evaluation of the degree of crystallinity

X- ray diffraction spectra for chitosan, PLA, and BSA coated on PLA coated chitosan MN arrays were recorded using Brucker D8 Advanced X-ray diffractometer (PDXL2 software, Tokyo, Japan) using Cu K 2α rays with a voltage of 40 kV and a current of 25 mA. Samples were scanned at the rate of 2 °ɵ from 10 to 60 °ɵ.

2.4.3.5 Determination of viscosity of wax mixture

A Rheometer (RVDV-II, Brookfield, USA) was used to study viscosity of wax and chitosan gel. The temperature control was achieved using heated plate, allowing temperature gradually increasing from 20 ^{0}C to 80 ^{0}C.

2.4.3.6 Determination of swelling index of microneedles array

A microneedles patch of 1 cm^2 (36 MN) size from optimized batch was weighed and placed on a pre-weighed cover slip. It was placed in a petridish and 10 mL of Distilled water was added. After 10 min, the cover slip was removed, and excess water was wiped off carefully using the tissue paper and weighed. Weight increase due to absorption of water and swelling of patch was determined by difference between initial and final weight.

The percentage swelling index was calculated using the following equation: 2

$$\% \text{ Swelling index} = (Wt - Wo / Wo) \times 100 \quad \text{----------(2)}$$

Where, Wt is final weight of the swollen film after time t, Wo is the initial weight of film at zero time.

2.4.3.7 BSA release study from microneedle array

Standard calibration curve of BSA was prepared by dissolving 10 mg of BSA in 100 mL phosphate buffer pH 7.4 to yield 100 µg/mL stock solution. From the stock solution further dilutions were made, viz 2, 4, 6, 8, 10, 20, 30, 40, 50 µg/mL respectively with phosphate buffer pH 7.4. From each dilution 1 mL of the solution was pipetted out and 2 drops of biuret reagent was added to it followed by dilution of the solution up to 3 mL with phosphate buffer. The reaction of BAS with biuret reagent generates pink or purple colouration which is observed and analysed in UV-Visible spectrophotometer (Shimadzu, Japan 1700) against Phosphate buffer as blank at 540 nm λ_{max}. These absorbance values were used to prepare the standard calibration curve of BSA.

The drug release studies of BSA coated microneedle arrays were performed by using Franz diffusion cell apparatus by using 45 mL of phosphate buffer pH 7.4 as dissolution medium at 37 ± 0.5 ^{0}C. The speed of magnetic stirrer was adjusted to 100 rpm. The microneedle arrays were inserted to the shaved rat skin fixed to the receiver compartment. From this compartment 1 mL of the medium was collected at a specific time interval and analysed for the content of BSA following the same protocol (biuret test) used to form BSA standard calibration curve. An equivalent volume (1 mL) of the fresh phosphate buffer was added to Franz diffusion cell apparatus each time to make up the loss due to sampling.[36]

2.4.3.8 Skin irritation study

Skin irritation study of MNs arrays were performed to determine whether the prepared MN arrays cause any irritation to the rat skin (Animal ethical committee approval no DYPIPSR/IAEC/Nov./18-19/P-09). MN arrays (1 cm x 3 cm) were applied by using gentle pressure to shaved back skin of Albino Wistar rats (180-220 gm) and secured for 24 hrs with medical adhesive tape. After 24 hrs MN arrays were removed and the rats were monitored for any sign of irritation on the rat's skin or any other adverse effects. The test site was analysed for 7 days post removal of the MN.[37]

3. Result and Discussion

3.1 Fabrication of wax Mould

The bees wax was melted at 63 ^{0}C and allowed to set in petridish for 30 min. The impression of Derma Roller® (1 mm needle length) was easily done to give MN mold. For fabrication of microneedles four different concentrations of chitosan were used. The various batches which were tried are given in Table 1.

Insert Figure 1 here

3.2 Optimization batches of microneedle patch.

The optimized batch (Batch D) was selected as 3% w/v chitosan prepared in 1% v/v acetic acid solution based on the mechanical strength and morphology of MNs (Table 1). This optimized batch was further coated with PLA (Batch E) and then with BSA (Batch F).[38-41]

Insert Table 1 here

3.3 Physical characterization of microneedle

3.3.1 Physical examination of microneedle array using Scanning Electron Microscopy (SEM).

A) Scanning electron microscopy

The normal and SEM images of plain chitosan MN, PLA coated chitosan MN and BSA coated on PLA coated MN arrays are shown in (Fig. 2). It can be clearly observed that 0.5 % chitosan MN appear thread like and has very less mechanical strength (Fig. 2a). Whereas, the 3% chitosan MN are formed nicely but with porous structure inside (Fig. 2b). When these 3% chitosan MNs were coated with PLA the MN became stronger with improved mechanical strength (Fig. 2c) and Fig. 2d suggest uniform coating of BSA over a PLA coat.[42] Moreover the SEM images suggest that the MNs are 0.9 mm in height, 600 µm in width at base, 30-60 µm at the tip diameter and the distance between two MN is 1.5 mm.[43]

Insert Figure 2 here

3.2.2 Mechanical strength of MNs arrays

Mechanical strength of microneedle needs to be enough to sustain the force applied during pressing of MN array patch into the skin.[44] This insertion compression force might lead to bending or breaking of MNs. The reported mechanical strength for efficient chitosan MNs was 0.50 N/needle.[45] and the mechanical strength of BSA and PLA coated chitosan MN was found to be 0.72 N/needle.

3.2.3 Tensile strength of MNs arrays

Tensile strength of MN arrays is important property as it defines the integrity of the patch and capacity of the patch to survive the physical stress. Previous reported tensile strength for

chitosan film was 11.23 Mpa[46] and the BSA and PLA coated MN array patch shows 15.23 Mpa.

3.2.4 Spectral and thermal analysis of MNs Arrays

3.2.4.1 FTIR spectroscopy

The FTIR spectrum of chitosan (Fig.3a) showed important bands of the characteristics functional groups which were recorded in the infrared range (4000 -600 cm^{-1}). The infrared spectra for chitosan showed the stretching vibration band at 3419.42 cm^{-1} for the OH group and band at 1064.79 cm^{-1} was associated with -C-O stretching vibration of CH_2OH group. Spectra also showed NH bend at 1643.41 cm^{-1} and NH stretch at 3354.15 cm^{-1} for amine group. The FTIR spectra of PLA (Fig.3b) showed 2839.73 cm^{-1} and 2910.68 cm^{-1} for C-H stretch and 1491.02 cm^{-1} C-H bending vibrations in CH_3 , OH stretch at 3464.23 cm^{-1}, C=O stretch at 1757.84 cm^{-1} and C-O-C stretching vibration were observed at 1350.32 cm^{-1}. The FTIR spectre of Plain BSA (Fig.3c) showed C=O stretch vibrations of the peptide linkages at 1667.21 cm^{-1}, N-H bending vibration for amide II at 1537.91 cm^{-1} and N-H bending vibration at 3292.60 cm^{-1}. The FTIR spectra of BSA and PLA coated chitosan microneedle (Fig.3d) showed all the characteristic peak of chitosan like of NH bend (amine) at 1635.41 cm^{-1} and NH stretch at 3249.20 cm^{-1}, 2930.93 cm^{-1} for C-H stretch and 1498.74 cm^{-1} C-H bending vibrations in CH_3 for PLA and for BSA N-H bending vibration for amide II at 1525.74 cm^{-1}, C-N stretching/bending vibration at 1166.97 cm^{-1} / 2330.34 cm^{-1} for BSA. Thus all the molecules retainsed their functional group and no interaction was observed between them.

Insert Figure 3 here

3.2.4.2 Thermal analysis of MN array

Insert Figure 4 here

DSC Thermogram of PLA (Fig.4a) show endothermic peaks at 56 ^{0}C and 105 ^{0}C related to glass transition (GT) and moisture loss and broad endothermic peak at 170 ^{0}C followed by broad exothermic peak at 220 ^{0}C is melting followed by degradation of PLA. These values match closely with previously reported value.[47] DSC thermogram of chitosan (Fig.4b) show endothermic peak at 90 ^{0}C related to moisture loss, endothermic peak at 240 ^{0}C followed by exothermic peak at 280 ^{0}C corresponds to degradation of chitosan. These values match closely with previously reported value.[48] The DSC thermogram of PLA coated chitosan microneedle (Fig.4c) shows small endothermic peak at 60 ^{0}C for GT of PLA, endothermic peak of water loss at 100 ^{0}C and endothermic peak at 230 ^{0}C followed by exothermic peak at 270 ^{0}C represents the degradation of PLA and chitosan respectively. The DSC thermogram of BSA and PLA coated microneedle (Fig.4d) shows short endothermic peak for GT of PLA at 63 ^{0}C and a short endothermic peak at 100 ^{0}C related to water loss and degradation of BSA.[49] A small exothermic peak at 215 ^{0}C corresponding to degradation of PLA and broad endothermic peak at 215 ^{0}C followed by 260 ^{0}C broad exothermic peak correspond to chitosan and PLA degradation.

3.2.4.3 XRD spectral analysis

Insert Figure 5 Here

The diffractogram of chitosan shows sharp peak at 22 °ɵ, 26.5 °ɵ and 33 °ɵ broad peak shows chitosan slightly crystalline in nature (Fig.5a). These observations match with previous reports.[21,48] The diffractogram of PLA shows broad peak at 16.55 °ɵ and 30 °ɵ. It suggests

that PLA used is amorphous in nature (Fig.5b) this observation match with reported value[50] and supports the DSC data which lack sharp endothermic peak of glass transition temperature at 60 ^{0}C. The diffractogram of BSA coated on PLA coated chitosan MN array batch (Fig. 5c) displayed sharp peak at 22 °ɵ, 24 °ɵ and 32 °ɵ emerging from a broad peak correspond to chitosan and broadness of the overall diffractogram correspond to PLA which suggests that coating of chitosan MN do not hamper crystallinity to the MN array. This is important observation as it explains improved mechanical properties of the MN array.

3.2.4.4 Drug Release profile of optimized batch

The *in-vitro* drug release study was carried out in order to ensure a release of drug in selected dissolution medium. The drug release profile was determined in phosphate buffer pH 7.4, 98.5 % BSA was released within 50 hours from rat skin (Fig. 6).[51]

Insert Figure 6 here

3.3 Determination of viscosity of wax and gel

The change of viscosity with increasing temperature gradient was performed for bee's wax and chitosan gel. The viscosity decreased with increase in temperature. Thus, both gel and wax come under the Newtonian flow behaviour.

3.4 Swelling index of microneedles arrays

Insert Figure 7 here

Figure 7 shows the swelling behaviour of the BSA and PLA coated MN array. It was observed that the maximum swelling of 6.79 % was observed at 30 minutes. After 30 minutes the weight decreased, it might be due to the dissolution of BSA.

3.5 In vivo tolerance study

After removal of MN and careful observation for next 7 days it was noted that there was no sign of irritation and any adverse effect due to MN (Fig. 8).

Insert Figure 8 here

4. Conclusion

The successful fabrication of microneedle was carried out using chitosan polymer and bees wax mould. Selected MN batch was subjected to coating with PLA and BSA, followed by morphological, mechanical, and drug release studies. Based on scanning electron microscopy characterization of microneedle formulation; the coated MNs were with 0.9 mm length, 600 µm width at the base, 1.5 mm distance between two needles and 30-60 µm tip diameter. The optimized MN batch showed the percent BSA release of 98.5 % in 50 hour. It also showed good mechanical strength (0.72 N/Needle), tensile strength 15.23 Mpa and maximum swelling of 6.79 %.

The results obtained from various studies performed for PLA and BSA coated layered chitosan MNs possessed desired mechanical strength, tensile strength, swelling index, and drug release. SEM, XRD and DSC studies established the physicochemical properties of microneedle.

Thus, it is concluded that the study of fabrication of novel wax-based mould (which can be melted and re-casted multiple times) and development of BSA and PLA coated chitosan microneedle was successfully attempted. The microneedle patches easily pierced the skin with gentle application of force. It showed significant amount of drug release to dermis.

Further, it is also proposed that the Wax based mould technique for the development of microneedle patch and the developed coated polymeric microneedles can be tested for its drugs, macromolecules and vaccines delivery potential as pain less and effective drug delivery system.
The same MN arrays can act as time-controlled delivery system as porous chitosan will be exposed after the dissolution of two layers (BSA and PLA). Thus, chitosan MN can be loaded with the drugs to be released after a particular time. Even PLA can be doped with certain medicament to obtain sustained drug delivery after the dissolution of BSA layer. BSA can be substitute with vaccines or DNA/RNA, to get the immediate release. Thus, each layer of MN will provide the platform for time bound drug delivery system.

5. Reference

1. Gualeni B, Coulman SA, Shah D, Eng PF, Ashraf H, Vescovo P, Blayney GJ, Piveteau LD, Guy OJ, Birchall JC. Minimally invasive and targeted therapeutic cell delivery to the skin using microneedle devices. British Journal of Dermatology. 2018;178:731-739.
2. Ita K. Transdermal Delivery of Drugs with microneedles—potential and challenges. Pharmaceutics. 2015;7:90–105.
3. Akhtar NA, Pathak K. Preclinical and clinical aspects of antimicrobial drugs delivered via ethosomal carriers. Antiinfective Ag. 2012;10:15-25.
4. Mishra R, Pramanick B, Maiti TK, and Bhattacharyya TK. Glassy carbon microneedles—new transdermal drug delivery device derived from a scalable C-MEMS process. Microsystems & Nanoengineering. 2018;4:1-11.
5. Hao Y, Li W, Zhou X, Yang F, Qian Z. Microneedles-Based transdermal drug delivery systems: A Review. J Biomed Nanotechnol. 2017;13:1581-1597.
6. Mansoor I, Lai J, Lambert D, Dutz J, Häfeli U, Stoeber B. Hollow metallic microneedles for transdermal drug delivery. Transactions of Japanese Society for Medical and Biological Engineering. 2013; 51(Supplement): M-38.
7. Nguyen J, Ita KB, Morra MJ and Popova IE. The Influence of solid microneedles on the transdermal delivery of selected antiepileptic drugs. Pharmaceutics. 2016;8:33.
8. Prausnitz MR. Engineering microneedle patches for vaccination and drug delivery to skin. Annual Review of Chemical and Biomolecular Engineering. 2017;8:177-200.
9. Kim KS, Ita K, Simon L. Modelling of dissolving microneedles for transdermal drug delivery: theoretical and experimental aspects. Eur. J. Pharm. Sci. 2015;68:137-143.
10. Jepps OG, Dancik Y, Anissimov YG, Roberts MS. Modeling the human skinbarrier-Towards a better understanding of dermal absorption. Adv. Drug Deliv. Rev. 2013;65:152-168.
11. Jacoby E, Jarrahian C, Hull HF, Zehrung D. Opportunities and challenges in delivering influenza vaccine by microneedle patch. Vaccine. 2015;33:4699-4704.
12. Ameri M, Kadkhodayan M, Nguyen J, Bravo JA, Su R, Chan K, Samiee A, and Daddona PE. Human growth hormone delivery with a microneedle transdermal system: Preclinical formulation, stability, delivery and PK of therapeutically relevant doses. Pharmaceutics 2014;6:220-234.
13. Jin X, Zhu DD, Chen BZ, Ashfaq M, Guo XD. Insulin delivery systems combined with microneedle technology. Send to Adv Drug Deliv Rev. 2018;127:119-137.
14. Kwon KM, Lim SM, Choi S, Kim DH, Jin HE, Jee G, Hong KJ, and Kim JY. Microneedles: quick and easy delivery methods of vaccines. Clin Exp Vaccine Res. 2017;6:156-159.
15. Huang D, Zhao D, Huang Y, Liang Z, Li Z. Microneedle roller electrode array (M-REA): A new tool for in vivo low-voltage electric gene delivery. In2018 IEEE Micro Electro Mechanical Systems (MEMS). 2018: 400-403.

16. Narayanan SP and Raghavan S. Solid silicon microneedles for drug delivery applications. The International Journal of Advanced Manufacturing Technology. 2017;93:407–422.
17. Rouhi N, Jung-Kubiak C, White V, Wilson D, Anderson J, Marrese-Reading C, Forouhar S. Fabrication of 3-D silicon microneedles using a single-step DRIE process. Journal of Microelectromechanical Systems. 2015;24:1409-1414.
18. Ullah A, Kim CM, and Kim GM. Porous polymer coatings on metal microneedles for enhanced drug delivery. R Soc Open Sci. 2018;5:171609.
19. Li J, Liu B, Zhou Y, Chen Z, Jiang L, Yuan W, Liang L. Fabrication of a Ti porous microneedle array by metal injection moulding for transdermal drug delivery. PLoS ONE. 2017;12:e0172043
20. Larrañeta E, Lutton REM, Woolfson AD, Donnelly RF. Microneedle arrays as transdermal and intradermal drug delivery systems: Materials science, manufacture and commercial development. Materials Science and Engineering: R: Reports. 2016;104:1-32.
21. Badhe RV, Nanda RK, Chejara DR, Choonara YE, Kumar P, du Toit LC, Pillay V. Microwave-assisted facile synthesis of a new tri-block chitosan conjugate with improved mucoadhesion. Carbohydrate polymers. 2015;130:213-221.
22. Samant PP, Prausnitz MR. Mechanisms of sampling interstitial fluid from skin using a microneedle patch. Proceedings of the National Academy of Sciences. 2018;115:4583-4588.
23. Wang M, Hu L, Xu C. Recent advances in the design of polymeric microneedles for transdermal drug delivery and biosensing Lab Chip. 2017;17:1373-1387.
24. Nejad HR, Sadeqi A, Kiaee G and Sonkusale S. Low-cost and cleanroom-free fabrication of microneedles. Nature Microsystems & Nanoengineering volume, 2018;4:17073.
25. Ono A, Ito S, Sakagami S, Asada H, Saito M, Quan YS, Kamiyama F, Hirobe S, and Okada N. Development of novel faster-dissolving microneedle patches for transcutaneous vaccine delivery. Pharmaceutics. 2017;9:27.
26. Waghule T, Singhvi G, Dubey SK, Pandey MM, Gupta G, Singh M, Dua K. Microneedles: A smart approach and increasing potential for transdermal drug delivery system. Biomedicine & Pharmacotherapy 2019;109:1249-1258.
27. Kang G, Tu TN, Kim S, Yang H, Jang M, Jo D, Ryu J, Baek J, Jung H. Adenosine□loaded dissolving microneedle patches to improve skin wrinkles, dermal density, elasticity and hydration. International journal of cosmetic science. 2018;40:199-206.
28. Naves L, Dhand C, Almeida L, Rajamani L, Ramakrishna S, and Soares G. Poly(lactic-co-glycolic) acid drug delivery systems through transdermal pathway: an overview. Prog Biomater. 2017;6:1–11.
29. Vora LK, Vavia PR, Larrañeta E, Bell SEJ, and Donnelly RF. Novel nanosuspension□based dissolving microneedle arrays for transdermal delivery of a hydrophobic drug. Journal of Interdisciplinary Nanomedicine. 2018;3:89-101.
30. Koen van der M, Sekerdag E, Schipper P, Kersten GFA, Jiskoot W, Bouwstra JA. Layer-by-Layer assembly of inactivated poliovirus and N-trimethyl chitosan on pH-sensitive microneedles for dermal vaccination. Langmuir: the ACS journal of surfaces and colloids. 2015;31:8654-8660.
31. Lin YH, Lee IC, Hsu WC, Hsu CH, Chang KP, and Gao SS. Rapid fabrication method of a microneedle Mould with controllable needle height and width. Biomedical Microdevices. 2016;18:85.
32. Fratini F, Cilia G, Turchi B, Felicioli F. Beeswax: A minireview of its antimicrobial activity and its application in medicine. Asian Pacific Journal of Tropical Medicine. 2016;9:839-843.

33. Lee K, Lee CY, Jung H. Dissolving microneedles for transdermal drug administration prepared by stepwise controlled drawing of maltose. Biomaterials. 2011;32:3134-3140.
34. Iliescu FS, Teo JC, Vrtacnik D, Taylor H, Iliescu C. Cell therapy using an array of ultrathin hollow microneedles. Microsystem Technologies 2018;24:2905-2912.
35. Badhe RV, Pradeep Kumar, Choonara YE, Thashree Marimuthu, du Toit LC, Divya Bijukumar, Chejara DR, Mostafa Mabrouk and Viness Pillay. Customized peptide biomaterial synthesis via an environment-reliant auto-programmer stigmergic approach. Materials. 2018;11:609.
36. Han T, Das DB. Permeability enhancement for transdermal delivery of large molecule using low-frequency sonophoresis combined with microneedles. J Pharm Sci. 2013;102:3614-3622.
37. Noh YW, Kim TH, Baek JS, et al. In vitro characterization of the invasiveness of polymer microneedle against skin. Int J Pharm. 2010;397:201-205.
38. Chen MC, Ling MH, Lai KY, Pramudityo E. Chitosan microneedle patches for sustained transdermal delivery of macromolecules. Biomacromolecules. 2012;13:4022-4031.
39. Sadeqi A, Nejad HR, Kiaee G and Sonkusale S. Cost-effective fabrication of chitosan microneedles for transdermal drug delivery," 2018 40th Annual International Conference of the IEEE Engineering in Medicine and Biology Society (EMBC), Honolulu, HI, 2018: 5737-5740.
40. Marin A and Andrianov AK. Carboxymethylcellulose–chitosan coated microneedles with modulated hydration properties. J. Appl. Poly. Sci. 2011;121:395-401.
41. Hong X, Wu Z, Chen L, Wu F, Wei L, Yuan W. Hydrogel microneedle arrays for transdermal drug delivery. Nano-Micro Lett. 2014;6:191-199.
42. Olatunji O, Igwe CC, Ahmed AS, Alhassan DO, Asieba GO, Diganta BD. Microneedles from fish scale biopolymer. Journal of Applied Polymer Science. 2014:131:40377.
43. Roxhed N, Gasser TC, Griss P, Holzapfel GA, Stemme G. Penetration enhanced ultra-sharp microneedles and prediction on skin Interaction for efficient transdermal drug delivery. Journal of Microelectromechanical Systems. 2007;16:1429-1440.
44. Olatunji O, Das DB, Garland MJ, Belaid L, Donnelly RF. Influence of array interspacing on the force required for successful microneedle skin penetration: Theoretical and practical approaches. J. Pharm. Sci. 2013;102:1209–1221.
45. Demir YK, Akan Z, Kerimoglu O. Sodium alginate microneedle arrays mediate the transdermal delivery of bovine serum albumin. PLoS ONE. 2013;8:e63819.
46. Justin R, Román S, Chen D, Tao K, Geng X, Grant RT, MacNeil S, Sunb K and Chen B. Biodegradable and conductive chitosan–graphene quantum dot nanocomposite microneedles for delivery of both small and large molecular weight therapeutics. RSC Adv. 2015;5:51934-51946.
47. Cao X, Mohamed A, Gordon SH, Willett JL and Sessa DJ. DSC study of biodegradable poly(lactic acid) and poly(hydroxy ester ether) blends. Thermochimica Acta. 2003;406:115–127.
48. Badhe RV, Bijukumar D, Chejara DR, Mabrouk M, Choonara YE, Pradeep Kumar, du Toit LC, Kondiah PPD and Pillay V. A Composite chitosan-gelatin bi-layered, biomimetic macroporous scaffold for blood vessel tissue engineering. Carbohydrate Polymers. 2017;3:1215-1225.
49. Luppi B, Bigucci F, Corace G, Delucca A, Cerchiara T, Sorrenti M, Catenacci L, Di Pietra AM, Zecchi V. Albumin nanoparticles carrying cyclodextrins for nasal delivery of the anti-alzheimer drug tacrine. European Journal of Pharmaceutical Sciences. 2011 Nov 20;44:559-65.

50. Giita Silverajah VS, Ibrahim NA, Yunus WM, Hassan HA, Woei CB. A comparative study on the mechanical, thermal and morphological characterization of poly(lactic acid)/epoxidized Palm Oil blend. Int J Mol Sci. 2012;13:5878-5898.
51. Gupta J, Gill HS, Andrews SN, Prausnitz MR. Kinetics of skin resealing after insertion of microneedles in human subjects. J. Control. Release. 2011;154:148–155.

Table no. 1. MN batches prepared on the wax mould

Batch	Image	Composition	Observation
(A)	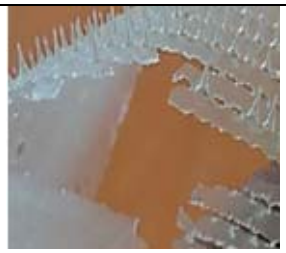	0.5% w/v chitosan 1% v/v acetic acid solution.	Arrays were brittle (TS* - 4.18 Mpa) and Needles formed were thread like with very less mechanical strength - 0.08 N/Needle).
(B)	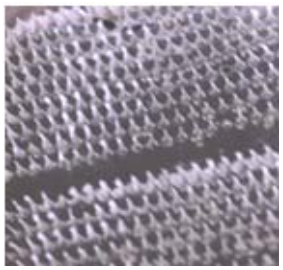	1%w/v chitosan in 1% in acetic acid solution	Microneedles were formed but short length (0.7mm) and less mechanical strength (0.15 N/Needle).
(C)		2%w/v chitosan in 1% v/v acetic acid solution.	Microneedles formed with optimum length but with less mechanical strength (0.28 N/Needle).
(D)	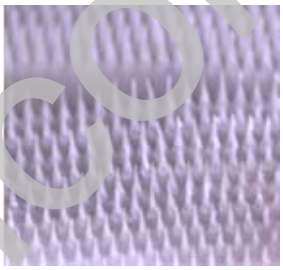	3%w/v chitosan in 1% v/v acetic acid solution.	Microneedles are formed with proper length and shape but with poor mechanical strength (0.53 N/Needle).
(E)		3% w/v chitosan in 1% v/v acetic acid MN coated with PLA	MNs arrays were formed with good length and strength (0.70 N/Needle) of needles.

(F)	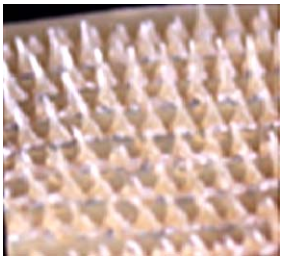	3% w/v chitosan in 1% acetic acid MN coated with PLA and BSA.	Needles were obtained with good length and mechanical strength (0.72 N/Needle).

* TS - tensile strength

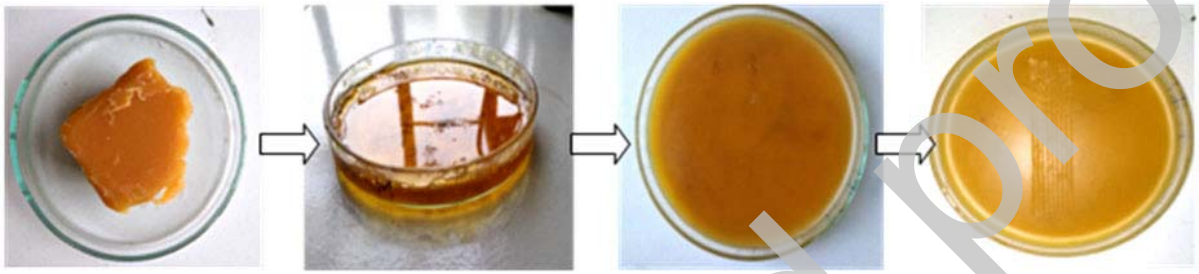

Figure 1.
Fabrication of wax-based MN array mould.

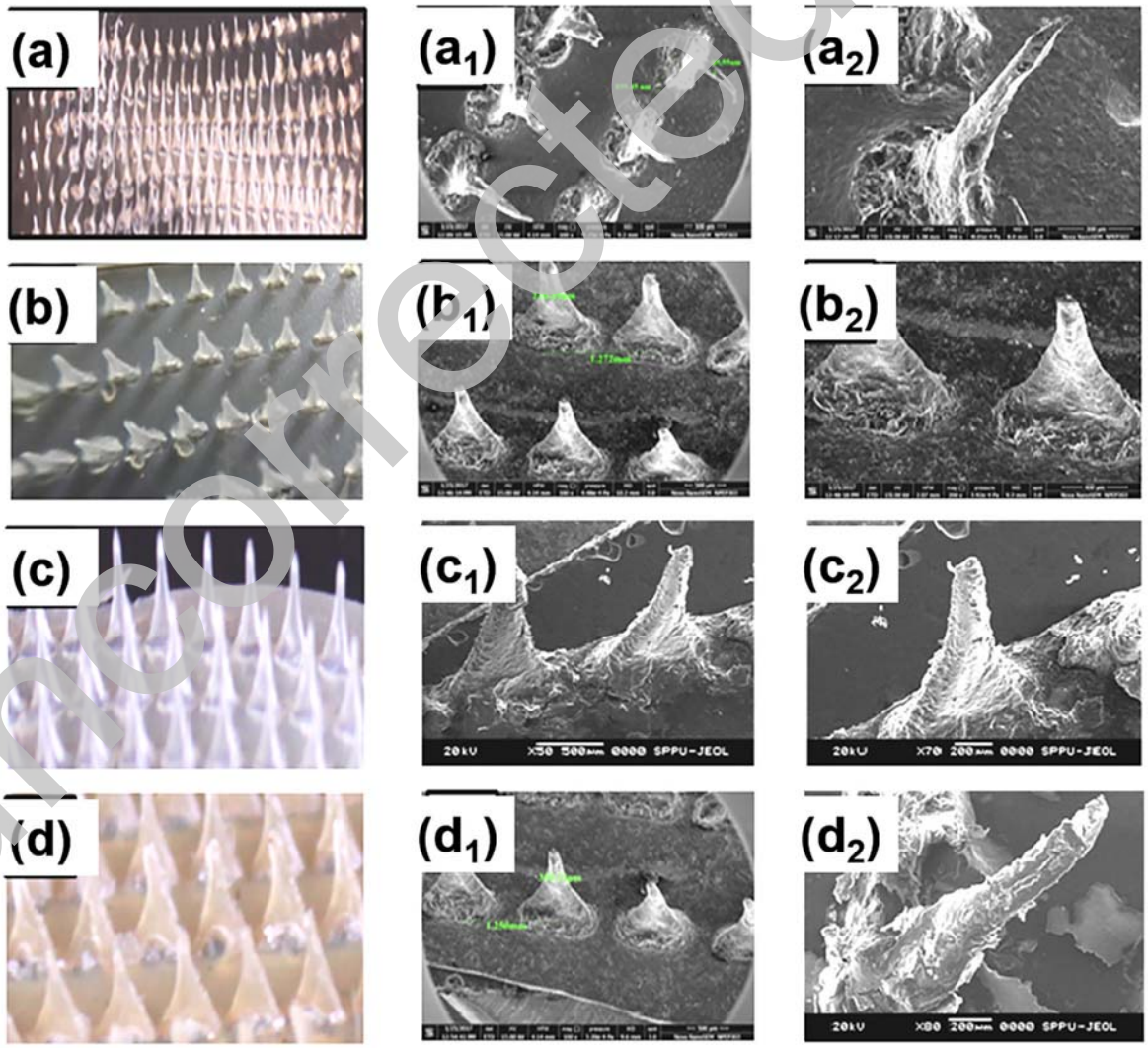

Figure 2.
SEM images of (a,a1,a2) 0.5_ chitosan MN (b,b1,b2) 3_ chitosan MN (c,c1,c2) PLA coated chitosan MN and (d,d1,d2) BSA coated on PLA coated chitosan MN array

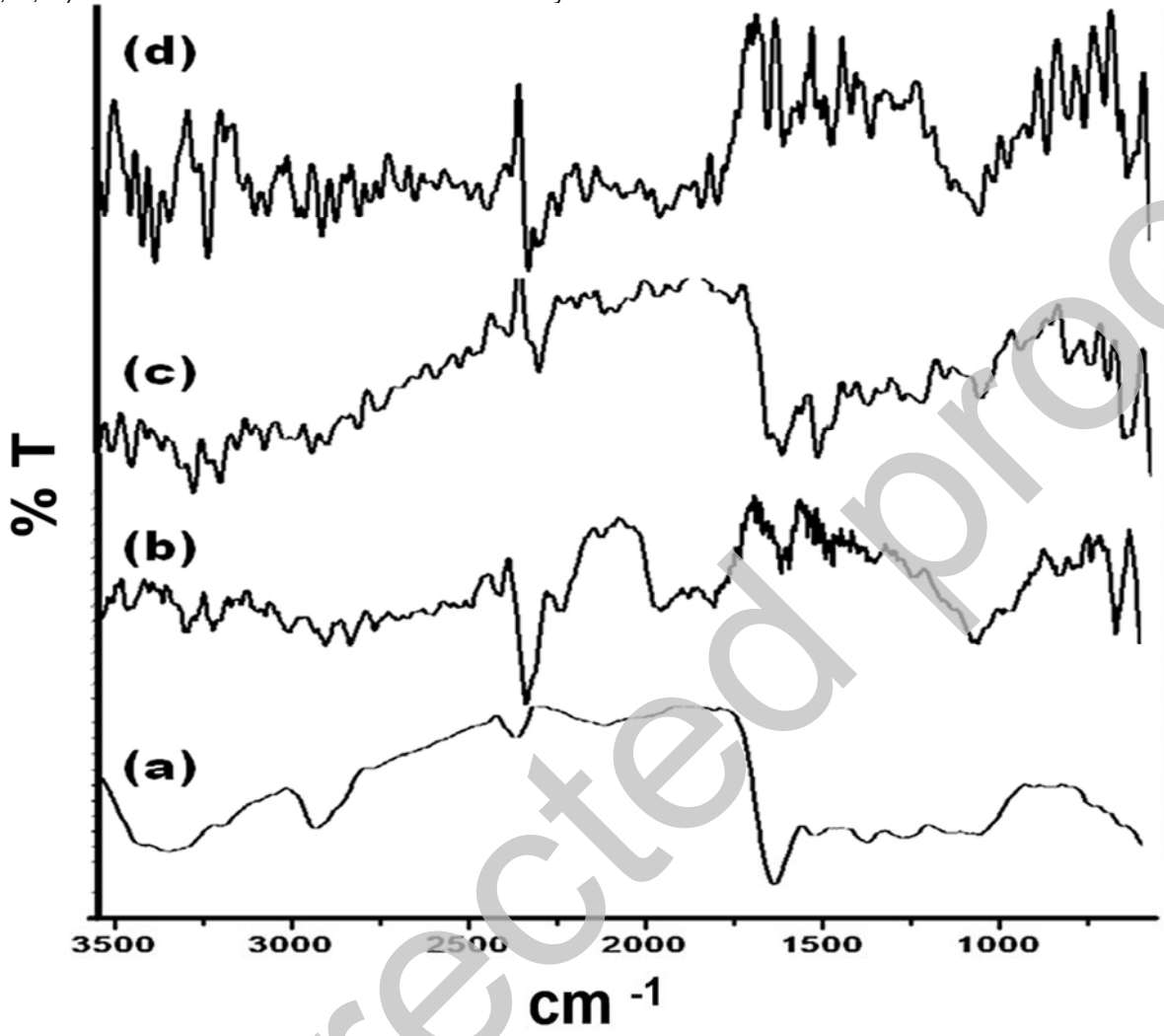

Figure 3.
FTIR spectra of a) chitosan b) PLA c) BSA and d) BSA coated on PLA coated chitosan MN array

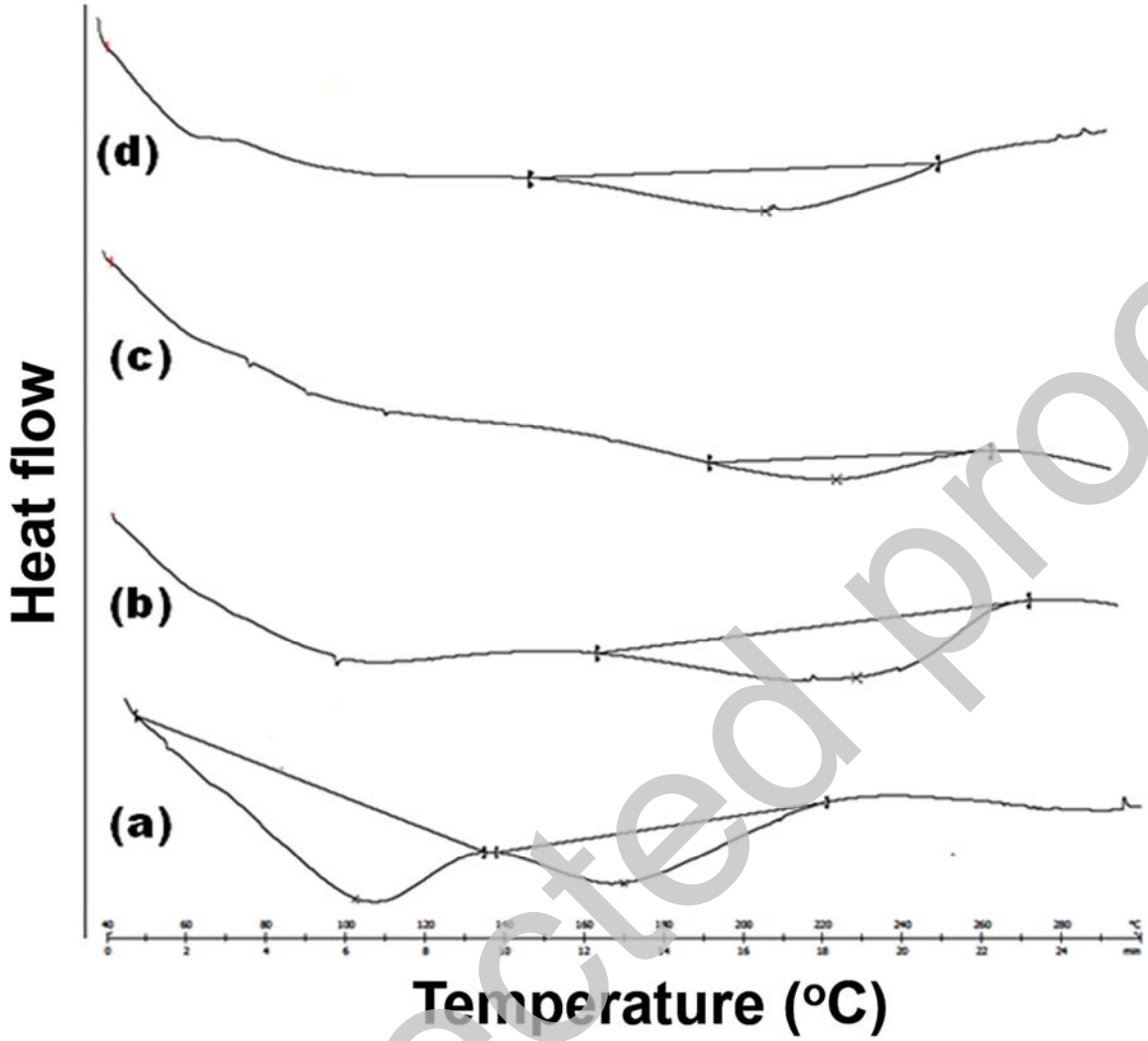

Figure 4.
DSC Thermogram of a) PLA b) chitosan c) PLA coated chitosan MN d) BSA coated on PLA coated chitosan MN array

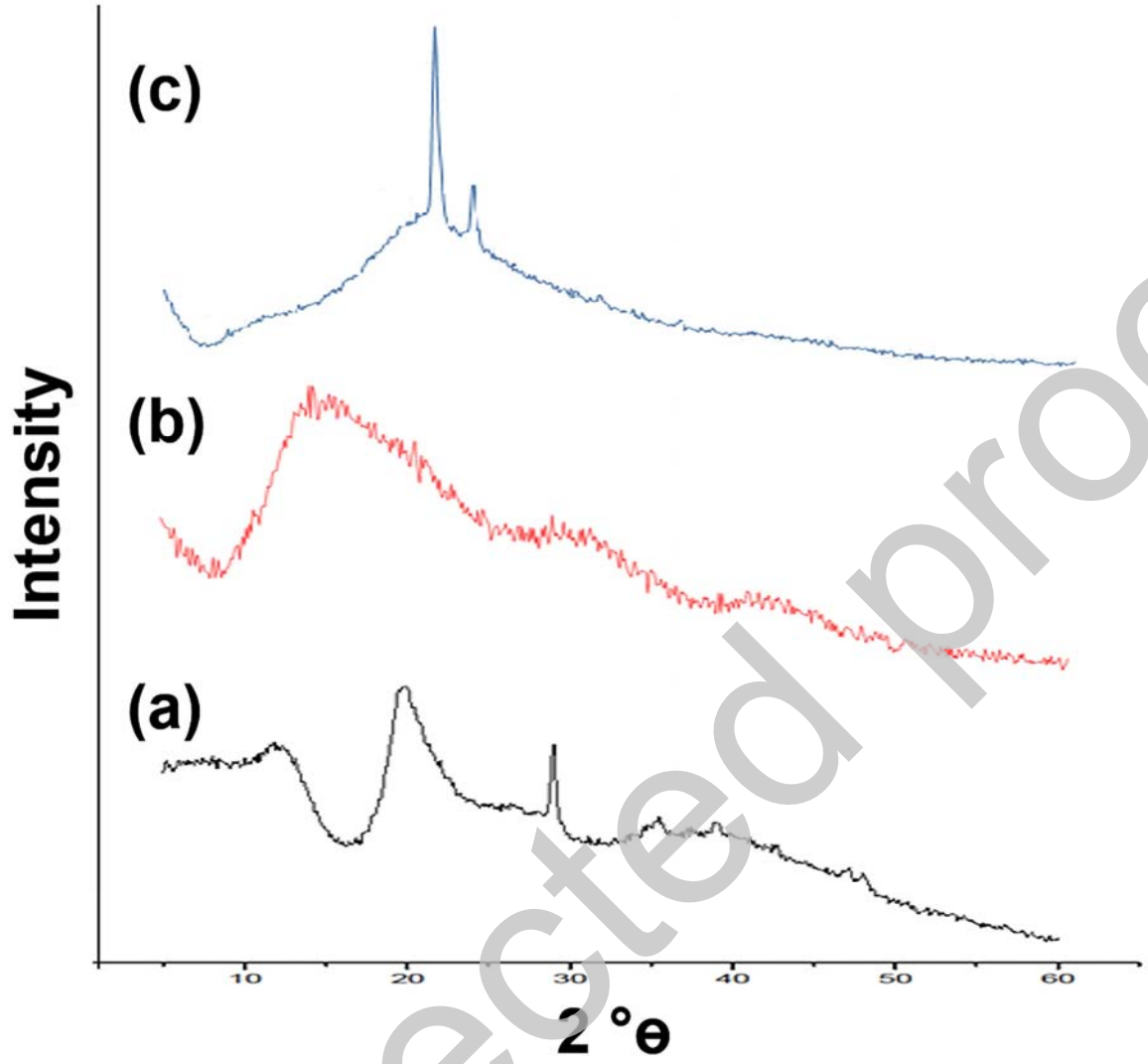

Figure 5.
XRD spectral analysis of a) chitosan b) PLA c) BSA coated on PLA coated chitosan MN array

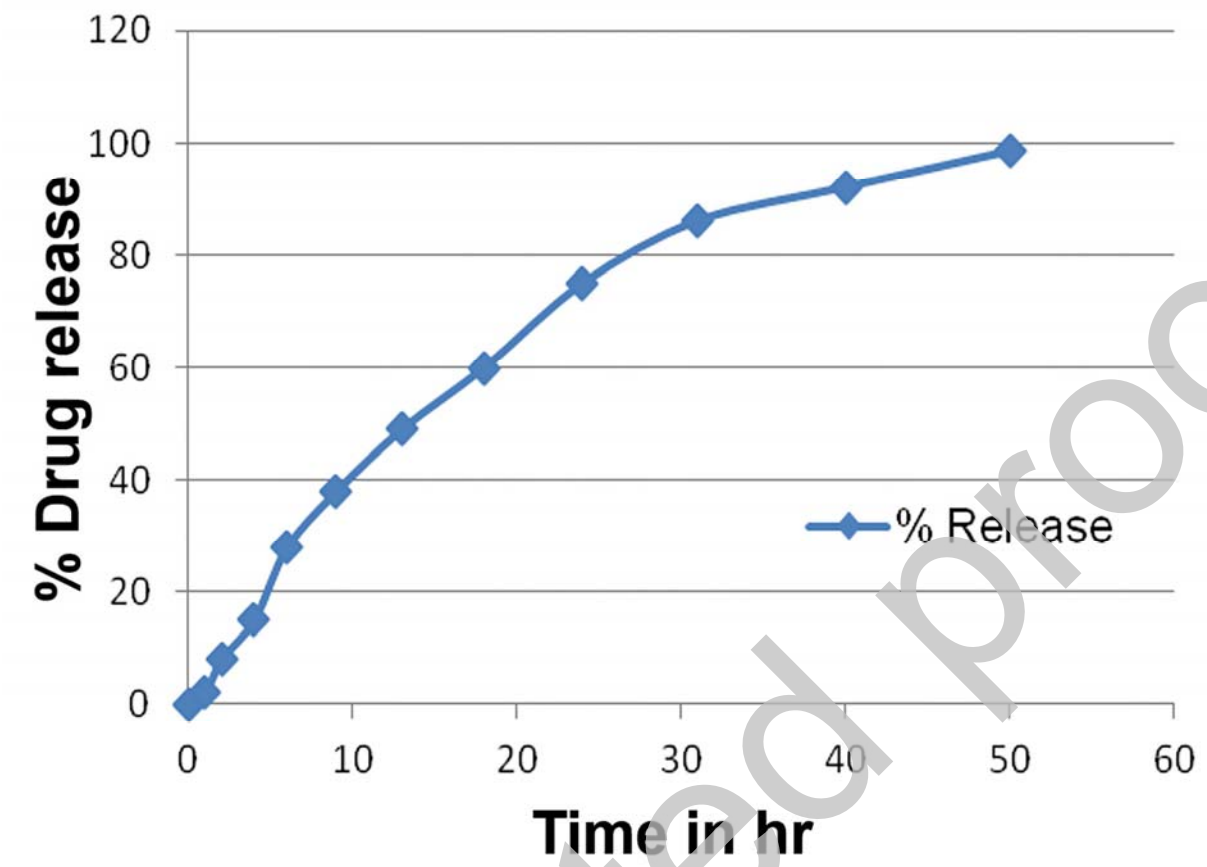

Figure 6.
_ Drug release of optimized batch

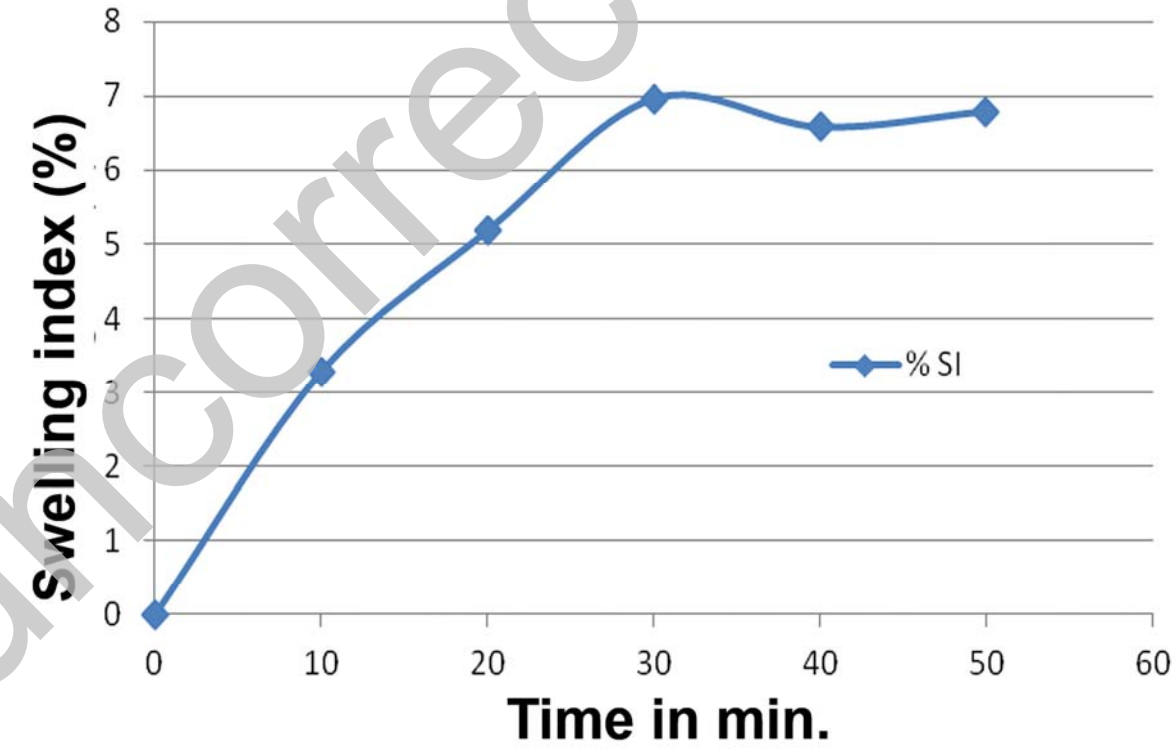

Figure 7.
Swelling index of BSA and PLA coated MN array

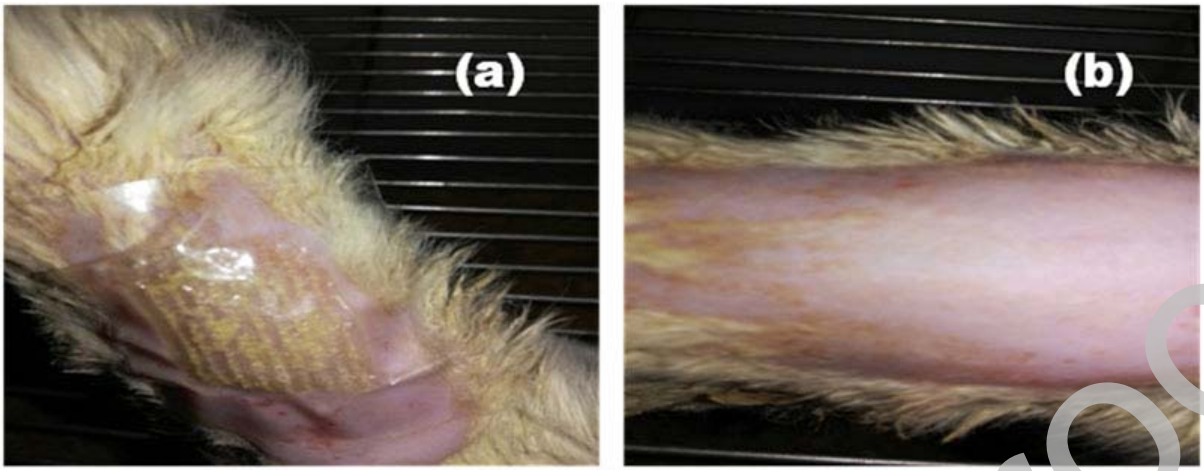

Figure 8.
Skin irritation study a) Microneedle array patch inserted in the Dorsal skin of rat b) Dorsal skin of rat after seven days of Microneedle array patch removal